Polarization rotation transitions in anisotropically strained $SrTiO_3$ thin films

A. Vasudevarao,[a] Sava Denev, Michael D. Biegalski, Yulan Li, Long-Qing Chen, Susan Trolier-McKinstry, Darrell G. Schlom, and Venkatraman Gopalan[b]
Department of Materials Science and Engineering, The Pennsylvania State University, University Park, Pennsylvania 16802,USA

(Received 5 February 2008; accepted 18 April 2008; published online 15 May 2008)

Commensurately strained epitaxial $SrTiO_3$ thin films on a $GdScO_3$ substrate with anisotropic in-plane tensile strains of 1.46% and 1.59% were grown. By using optical second harmonic generation and polarization measurements, a ferroelectric transition from a tetragonal $4/mmm$ phase to a ferroelectric $mm2$ phase at ~400 K and an antiferrodistortive transition to a multiferroic phase at 150–175 K are observed, which are in agreement with thermodynamic calculations. In addition, a series of polarization rotation transitions between $\langle 100\rangle_p$ to $\langle l00\rangle_p$ $(0<l<1)$ is observed in the 4–400 K temperature range. © *2008 American Institute of Physics*. [DOI: 10.1063/1.2921789]

Strontium titanate ($SrTiO_3$) in its bulk form is centrosymmetric with the cubic point group $m\bar{3}m$ at room temperature and undergoes a structural transition to a tetragonal nonpolar $4/mmm$ phase when cooled below 105 K. Cooling to still lower temperatures results in a strong Curie–Weiss-type behavior in the dielectric response, which is suggestive of an incipient ferroelectric transition at ~20 K. However, this transition to a ferroelectric phase remains incomplete down to 0 K.[1,2] Thermodynamic[3,4] as well as first principles calculations[2] predict that application of biaxial compressive or tensile strain can make $SrTiO_3$ ferroelectric. These predictions have been confirmed by experiments in epitaxial, commensurately strained $SrTiO_3$ grown on various substrates, where the films become ferroelectric near room temperature.[5] They also undergo an octahedral tilt transition at low temperatures.[6,7] Phase-field simulations and experimental studies conducted on strained $(001)_p$ $SrTiO_3$ films have primarily focused on *uniform* biaxial strain, where the strain values along the $[100]_p$ and the $[010]_p$ (where the subscript p indicates the pseudocubic Miller index) directions are equal. $GdScO_3$ substrates are orthorhombic with a $GdFeO_3$ crystal structure and *Pbnm* space group. Such substrates were used in this work with $(001)_o$ (o for orthorhombic notation) orientation that leads to an asymmetric in-plane growth net with lattice parameters of 3.964 ± 0.001 and 3.967 ± 0.001 Å.[8–10] This anisotropic strain state is only present in fully commensurate thin films and relaxes to a uniform in-plane strain state with increasing film thickness, as has been presented in previous publications.[3,5,6]

This letter focuses on the domain structure and phase transitions in an anisotropically strained 250 Å thick $SrTiO_3$ film grown on a $GdScO_3$ substrate. Reactive molecular beam epitaxy was used to grow an epitaxial $SrTiO_3$ film on a $(110)_o$ oriented $GdScO_3$ substrate. X-ray diffraction scans show that on this substrate, $SrTiO_3$ grows with an in-plane lattice constant of 3.962 ± 0.001 Å (tensile strain of 1.46%) along the $[100]_p$ direction and 3.967 ± 0.001 Å (tensile strain of 1.59%) along the $[010]_p$ direction (referred to as the short and long axes, respectively) and an out-of-plane lattice constant of 3.872 ± 0.001 Å (compressive strain of 0.85%). The film is fully commensurate with the substrate, within the accuracy of the measurements. The film under study was of excellent crystalline quality, with the full width at half maximum in the rocking curve of the $[002]_p$ $SrTiO_3$ peak being 0.0025°. Thermodynamic calculations similar to the procedure outlined in Ref. 3 were performed for a $SrTiO_3$ film on a $GdScO_3$ substrate subject to biaxial strains of 1.46% along $[100]_p$ and 1.59% along $[010]_p$. Calculations predict that the transition from the paraelectric to the ferroelectric state occurs at 393 ± 81 K, wherein the error range is due to the variations in the reported electrostrictive coefficients. Below the transition temperature, the ferroelectric polarization develops along the $[010]_p$ direction. Upon cooling to below 355 ± 77 K, the polarization develops components along both the in-plane directions, as shown in Fig. 1. As it is cooled further, at around 147 ± 29 K, $SrTiO_3$ undergoes an antiferrodistortive transition, which is characterized by an order parameter $\mathbf{q}=(q_1,q_2,0)$, which is proportional to the rotation angle ζ of the oxygen octahedra, which is given by $q_1=(a/2)\tan\zeta$ and $q_2=(b/2)\tan\zeta$, where a and b refer to the lattice parameters of $SrTiO_3$ in the antiferrodistortive phase. Below 147 ± 29 K, $SrTiO_3$ shows both antiferrodistortive and ferroelectric order parameters.

In order to verify these predictions, optical second harmonic generation (SHG) and ferroelectric polarization measurements[11,12] were employed. SHG involves the conversion of light (electric field E^{ω}) at a frequency ω through the creation of a nonlinear polarization $P_i^{2\omega}\propto d_{ijk}E_j^{\omega}E_k^{\omega}$.[13] The fundamental wave of 800 nm was incident from the substrate side in normal geometry. The sample was placed inside a cryostat allowing the temperature to be varied from 4 to 400 K. A reference study of bare (110) $GdScO_3$ without any film yielded no SHG within detection limits. The polarization direction of incident light, which is at an angle θ from the x axis, was continuously rotated within the plane of the film [see Fig. 2(a)]. The intensity $I_j^{2\omega}$ of the output SHG signal at a 400 nm wavelength was detected along either the $j=x\equiv[100]_p$ or $y\equiv[010]_p$ directions by a photomultiplier tube. The resulting polar plots of the SHG intensities $I_x^{2\omega}(\theta)$ and $I_y^{2\omega}(\theta)$ at 338 K are shown in Fig. 2.

In accord with the thermodynamic and first-principles predictions,[2–4] the $mm2$ point group was considered for the ferroelectric phase, wherein the twofold rotation axis lies

[a]Electronic mail: azv105@psu.edu.
[b]Electronic mail: vgopalan@psu.edu.

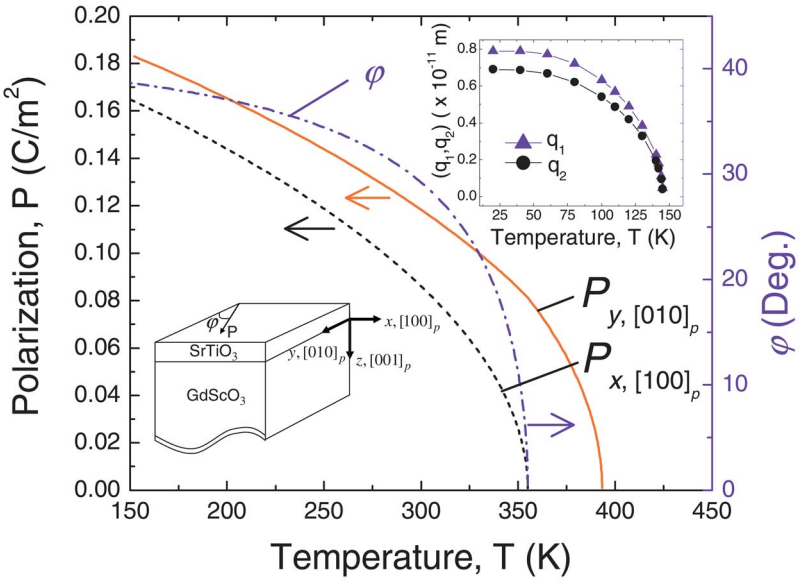

FIG. 1. (Color online) Thermodynamic predictions of variation in polarization with temperature for anisotropically strained $SrTiO_3$ on a $GdScO_3$ substrate. The solid (dashed) line represents $P_y(P_x)$, which is the component of ferroelectric polarization along the $y \equiv [010]_p$ ($x \equiv [100]_p$) directions. The dash-dot line represents the angle between the ferroelectric polarization in the material and the long axis $y \equiv [010]_p$. The inset graph (top right) shows the thermodynamic predictions of variation in antiferrodistortive order parameters q_1 and q_2 with temperature. The inset (bottom left) shows a schematic of the directions of polarization with respect to the $SrTiO_3$ directions.

within the plane of the $SrTiO_3$ thin film. By symmetry considerations, the ferroelectric polarization in this point group can lie only along the twofold rotation axis. A theoretical analysis of this film system similar to that outlined in other references,[11,14] yields the following expression for the SHG intensity:

$$I_j^{2\omega}(\theta) = K_{1,j}\sin^2 2(\theta-\varphi) + K_{2,j}[\sin^2(\theta-\varphi) + K_{3,j}\cos^2(\theta-\varphi)]^2 + K_{4,j}[\sin^2(\theta-\varphi) + K_{3,j}\cos^2(\theta-\varphi)]\sin 2(\theta-\varphi) \quad (1)$$

for angular offset φ between the x or y axis and the direction of ferroelectric polarization, and $K_{1,j}$, $K_{2,j}$, $K_{3,j}$, and $K_{4,j}$ are constants. By assuming a ferroelectric polarization along $y \equiv [010]_p$ *only*, it was not possible to fit the SHG data to Eq. (1) at *any* temperature. Then, we went on to assume that the ferroelectric polarization appears along both of the $\langle 100\rangle_p$ directions, i.e., due to domains. In this case, the model equation requires that we should be able to fit Eq. (1) to the data with $\varphi = 0°$. Also, calculations similar to that outlined in Ref. 3 require that $K_{3,x} = (K_{3,y})^{-1}$ *both* in magnitude and *sign*, which we call the *reciprocity condition*. In determining the value of $K_{i,j}$ from the nonlinear least square fitting of the experimental data to the model equations, care was taken to avoid local minima by starting from several different starting magnitudes and signs of the coefficients until convergence of a consistent set of $K_{i,j}$ was achieved. Furthermore, the material and microstructural properties obtained from the fit parameters $K_{i,j}$ were checked to make physical sense. It was found that with these constraints, it was not possible to fit the experimental data to the model with polarization along the $\langle 100\rangle_p$ directions at all temperatures. Thus, the constraint for the polarization direction was relaxed in order to allow the polarization to develop along an angle φ from both the $x \equiv [100]_p$ and $y \equiv [010]_p$ directions. The magnitude of the rotation angle φ was obtained from fitting the obtained SHG data to the model equation (1). Figure 2 shows the experimental data $I_x^{2\omega}(\theta)$ and $I_y^{2\omega}(\theta)$ obtained at $T = 338$ K. Figure 2(a) shows the fit of Eq. (1) to experimental data with φ as a free parameter, while Fig. 2(b) shows similar fits, with $\varphi = 0°$. The least square fit errors (reduced χ^2) in the case of $I_y^{2\omega}(\theta)$ Fig. 2(b) is 1.24, while in Fig. 2(a) it is significantly better (=0.0052). This shows that φ is an important parameter in fitting out data to model equation (1). We note that a different set of $K_{i,j}$ could give better fits even with $\varphi = 0°$; however, the reciprocity condition is then not satisfied, and hence the fits are invalid. Also, by assuming polarization directions along both the $\langle 100\rangle_p$ and $\langle 110\rangle_p$ in-plane directions, as well as more complex domain structure models, such as continuous distributions of polarization vector versus angle φ were considered. These latter models have more fit parameters and can always fit the obtained data. The goal was therefore to fit the polar plots with the simplest model with the least number of fitting parameters.

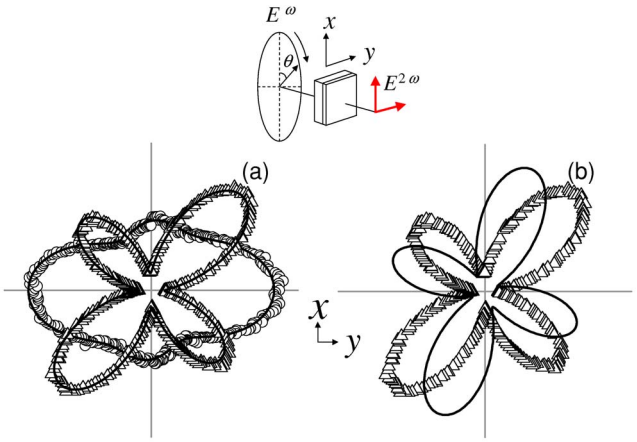

FIG. 2. (Color online) Polar plots of SHG intensities at $T = 338$ K, where the directions $x \equiv [100]_p$ and $y \equiv [010]_p$ are defined in the inset. (a) The circles (triangles) represent experimental data obtained for $I_x^{2\omega}(\theta)$ ($I_y^{2\omega}(\theta)$). The solid lines represent fits of experimental data to model equation (1) with φ as a free parameter. (b) Same experimental data $I_y^{2\omega}(\theta)$ as (a). The solid line represents fit to equation (1) with $\varphi = 0°$ and $K_{i,j}$ values fixed to be the same as (a).

Figure 3(a) shows the variation in SHG intensity with temperature in the following configuration: The fundamental light polarized along the short axis (x,$[100]_p$) and the intensity of the SHG signal was observed along the long axis (y,$[010]_p$). Upon cooling from higher temperatures, the SHG signal starts to increase at about 400 K. This is the ferroelectric transition temperature from the high temperature $4/mmm$ phase to the ferroelectric $mm2$ phase, which was predicted to

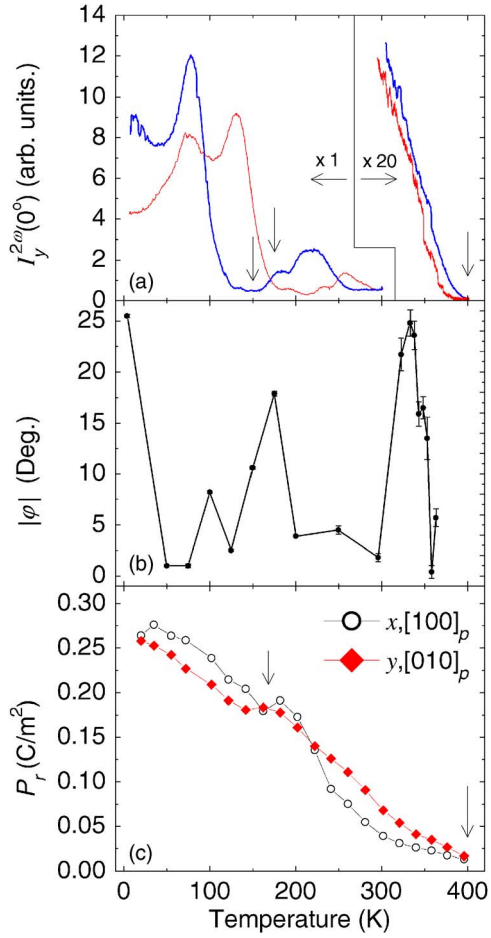

FIG. 3. (Color online) (a) Variation in SHG intensity $I_y^{2\omega}(0^\circ)$ with temperature during the heating [thin (red) solid line] and cooling [thick (blue) solid line] cycle. Note that the SHG intensities below and above 300 K are on different scales. The onset of ferroelectric phase transition (T=400 K) and antiferrodistortive phase transition during the heating (T=175 K) and cooling (T=150 K) cycle are highlighted by the vertical arrows. (b) Variation in magnitude of angular offset φ obtained from one measurement of $I_y^{2\omega}(\theta)$ with temperature. Multiple measurements confirm the trend. (c) Variation in remnant polarization in the film along the $x \equiv [100]_p$ [(black) open circles] $y \equiv [100]_p$ [(red) filled diamonds] directions with temperature, which were obtained from dielectric measurements. The onset of ferroelectric transition (T=400 K) and antiferrodistortive transition (T=160–180 K) is highlighted by the vertical arrows.

occur from thermodynamic calculation at $T_c \sim 393 \pm 81$ K. Measurement of remanent polarization from the polarization–electric field hysteresis loops in the material [Fig. 3(c)] also shows the onset of ferroelectric polarization along both the $x([100]_p)$ and $y([010]_p)$ directions at 400 K. This is also consistent with negligible values of angular offset φ in the temperature range of 358–363 K, as shown in Fig. 3(b). Upon further cooling below 358 K, the directions of ferroelectric polarization rotate from $\langle 100 \rangle_p$, as signified by an increase in the value of φ. The temperature ranges in which the polarization appears along the $\langle 100 \rangle_p$ in-plane directions can be readily identified in Fig. 3(b). As the material is cooled further, the directions of polarization switch back and forth between $\langle 100 \rangle_p$ and $\langle l10 \rangle_p$ down to 4 K. We note that in contrast, the phase-field theory performed here predicts only one switch from $\langle 100 \rangle_p$ to $\langle l10 \rangle_p$ $(0 < l < 1)$ *at* 355 ± 77 K and no reversal back. Furthermore, the polarization in the $\langle 100 \rangle_p$ polarization phase is predicted only along the "long" substrate axis, while experimentally, both SHG and electrical measurements indicate that polarization exists along both the $\langle 100 \rangle_p$ in-plane directions. These discrepancies are presently not understood, but are likely to be due to the uncertain temperature dependence of substrate lattice parameters and anisotropy. Upon further cooling, the SHG intensity shows a steep slope in the temperature range of 150–175 K. This coincides with the onset of antiferrodistortive transition (T_{AFD}) predicted by theory to be $T_{\mathrm{AFD}} = 147 \pm 29$ K. Polarization measurements [Fig. 3(c)] also show an anomaly in this temperature range (160–180 K).

In conclusion, commensurate anisotropically strained $[001]_p$ oriented $SrTiO_3$ thin films on a $(110)_o$ $GdScO_3$ substrate were grown. The ferroelectric and antiferrodistortive transitions are observed as predicted by theory. Interestingly, a repeated rotation of directions of ferroelectric polarization from the $\langle 100 \rangle_p$ to the $\langle l10 \rangle_p$ $SrTiO_3$ directions is observed with temperature. Figure 3(a) suggests that the $\langle 100 \rangle_p$ polarization phase dominates in most of the temperature range, while polarization temporarily rotates about $\langle 100 \rangle_p$ near "perturbations" to the film lattice, such as near T_c, near T_{AFD}, and at other (yet not understood) perturbations in the temperature ranges of 95–115 and 4–25 K. A complete thermodynamic prediction of this complex behavior will require the precise temperature dependence of substrate lattice parameters, particularly near these perturbations.

We wish to gratefully acknowledge financial support from National Science Foundation Grant Nos. DMR-0602986, 0512165, 0507146, and 0213623.

[1] K. A. Muller and H. Burkard, Phys. Rev. B **19**, 3593 (1979).
[2] A. Antons, J. B. Neaton, K. M. Rabe, and D. Vanderbilt, Phys. Rev. B **71**, 024102 (2005).
[3] Y. L. Li, S. Choudhury, J. H. Haeni, M. D. Biegalski, A. Vasudevarao, A. Sharan, H. Z. Ma, J. Levy, V. Gopalan, S. Trolier-McKinstry, D. G. Schlom, Q. X. Jia, and L. Q. Chen, Phys. Rev. B **73**, 184112 (2006).
[4] N. A. Pertsev, A. G. Zembilgotov, and A. K. Tagantsev, Phys. Rev. Lett. **80**, 1988 (1998).
[5] J. H. Haeni, P. Irvin, W. Chang, R. Uecker, P. Reiche, Y. L. Li, S. Choudhury, W. Tian, M. E. Hawley, B. Craigo, A. K. Tagantsev, X. Q. Pan, S. K. Streiffer, L. Q. Chen, S. W. Kirchoefer, J. Levy, and D. G. Schlom, Nature (London) **430**, 758 (2004).
[6] A. Vasudevarao, A. Kumar, L. Tian, J. H. Haeni, Y. L. Li, C.-J. Eklund, Q. X. Jia, R. Uecker, P. Reiche, K. M. Rabe, L. Q. Chen, D. G. Schlom, and V. Gopalan, Phys. Rev. Lett. **97**, 257602 (2006).
[7] S. Denev, A. Kumar, M. D. Biegalski, H. W. Jang, C. M. Folkman, A. Vasudevarao, Y. Han, I. M. Reaney, S. Trolier-McKinstry, C.-B. Eom, D. G. Schlom, and V. Gopalan, "Nonlinear optical probing of the color symmetry of octahedral rotations in strained $SrTiO_3$ thin films," Phys. Rev. Lett. (submitted).
[8] R. Uecker, P. Reiche, V. Alex, J. Doerschel, and R. Schalge, J. Cryst. Growth **137**, 278 (1994).
[9] R. P. Liferovich and R. H. Mitchell, J. Solid State Chem. **177**, 2188 (2004).
[10] M. D. Biegalski, S. Trolier-McKinstry, D. G. Schlom, S. K. Streiffer, R. Uecker, and P. Reiche, "Asymmetric dielectric properties of $SrTiO_3$ thin films on $DyScO_3$ substrates," J. Appl. Phys. (submitted).
[11] V. Gopalan and R. Raj, J. Appl. Phys. **81**, 865 (1997).
[12] M. Fiebig, V. V. Pavlov, and R. V. Pisarev, J. Opt. Soc. Am. B **22**, 96 (2005).
[13] Y. R. Shen, *The Principles of Nonlinear Optics* (Wiley, New York, 2003), p. 86.
[14] V. Gopalan and R. Raj, J. Am. Ceram. Soc. **79**, 3289 (1996).